Large-scale tests of 50-year-old prestressed concrete bridge girders

Received: 27 June 2025 | Revised: 20 December 2025 | Accepted: 19 January 2026

DOI: 10.1002/suco.70488

ARTICLE

fib CEB-FIP WILEY

Large-scale tests of 50-year-old prestressed concrete bridge girders

Francesco Tondolo[1] | **Pierclaudio Savino**[1] | **Donato Sabia**[1] | **Antonino Quattrone**[1] | **Fabio Biondini**[2] | **Gianpaolo Rosati**[2] | **Mattia Anghileri**[2] | **Bernardino Chiaia**[1]

[1]Department of Structural, Geotechnical and Building Engineering, Politecnico di Torino, Turin, Italy

[2]Department of Civil and Environmental Engineering, Politecnico di Milano, Milan, Italy

Correspondence
Francesco Tondolo, Department of Structural, Geotechnical and Building Engineering, Politecnico di Torino, Turin 10129, Italy.
Email: francesco.tondolo@polito.it

Funding information
SCR Piemonte S.p.A.

Abstract

An experimental investigation has been carried out as part of the BRIDGE|50 research project, focusing on large-scale loading tests performed on five 50-year-old prestressed concrete (PC) girders. The study aimed at evaluating the structural response of five girders retrieved from a viaduct in the urban area of Turin, Italy, subjected to 4-point bending tests with different levels of deterioration. The girders with a span of 19.2 m and an I-shaped cross section exhibited damage due to both dismantling phase operations and intentional cutting of some prestressing strands. The experimental activity defined the measurements of several critical parameters, such as load, deflections, and multiple strain values to capture bending and shear effects. This paper offers results of the structural performance of aged PC bridge girders both in service conditions and at collapse also in the presence of damage. The outcomes will increase the available knowledge on existing PC bridges, extending the database of large-scale tests that could be also used as a benchmark for numerical models aimed at developing more effective strategies for safety evaluation of existing bridges.

KEYWORDS

bridge girder, existing bridges, experimental test, large-scale, prestressed concrete girder

1 | INTRODUCTION

The management of existing bridges is a complex issue in civil engineering due to the challenges posed by deterioration phenomena affecting these important structures.[1] As critical components of our transport infrastructure, bridges are subjected to several threats that contribute to their progressive deterioration. Increased traffic loads, more frequent extreme events due to climate change, the corrosive effects of de-icing agents, inadequate maintenance programs, and poor structural detailing, also enhanced by poor-quality building materials, are all contributing to the deterioration of many bridges.[2,3] The combined result of structural deficiencies and functional obsolescence requires a thorough and global assessment, highlighting the importance of a multidisciplinary approach to bridge management in the civil engineering sector. In this context, field measurements and full-scale

experimental tests represent primary tools to inform mechanical and numerical models and ensure a more reliable safety assessment of existing bridges. Leveraging data derived from full-scale loading tests allows for the consideration of uncertainties that are representative of real bridge conditions experienced during service life. The creation of a wide database can enhance statistical information on structural performance of in-service bridges, refine structural models, and improve residual safety assessments. However, it must be pointed out that conducting full-scale tests on existing bridges is expensive and challenging, and this limits their usage. The BRIDGE|50 research project has been established with the aim of filling the gap in the field of experimental and numerical activities (www.bridge50.org). In this paper, the outcomes of five large-scale test and material testing are reported. In the following, a literature review of full-scale experimental tests conducted on bridge girders is reported.

In 1991, Shenoy and Frantz[4] investigated the effect of deterioration after 27 years of service on two PC box girders removed from the Walnut Street Bridge. The beams were tested with loads applied at third points to simulate HS-20 (1989 AASHTO) truck axle load. Both beams revealed lower prestressing losses than expected, higher cracking load and a level of residual stress in strands in line with the one obtained using ACI code. Azizinamini et al.[5] performed a structural test on a 25-year-old PC I-girder taken from a bridge near Lincoln, Nebraska, USA. The focus was addressed to the available prestress in the girder through a newly introduced stress method measured around a drilled hole. In addition, the ultimate load test was carried out using a four-point bending test setup with the applied loads at 1.8 m. Prestressing losses were lower than expected and behavior up to failure was monitored through strain gauges and transducers to reconstruct curvatures. Halsey and Miller[6] examined two portions of a 40-year-old bridge deck constituted by inverted PC T-beams and cast in situ concrete slab. At the time of decommissioning the bridge was in good structural condition. The specimens were subjected to a three-point bending test configuration until the top fiber of the section at midspan crushed under compression. The tests were intended to study cracking in service, loss of prestress and ultimate capacity at failure and compare it with current code provisions from AAASHTO. Pessiki et al.[7] conducted an experimental investigation on two PC bridge I-beams after 28 years of service. These beams were taken from the Shenango River Bridge in Pennsylvania, with a span length of 27.6 m. Both beams were tested in a three-point bending test configuration for both residual prestressing evaluation purposes and capacity at failure where concrete crushing in the compression zone was evidenced. Around 60% of estimated prestressing loss was measured through experimental tests. Eder et al.[8] tested two 50-year-old PC bridge girders 13.7 m long, made composite with a deck slab. The loading test was performed using a four-point bending test configuration with a shear span of about 5 m. During the loading test, the slab cracked and separated from the girders, highlighting ineffective composite behavior. Cracking during loading revealed that the girder was still able to support service loading without cracking. Pape and Melchers[9] investigated the structural performance of three PC post-tensioned beams recovered from the Sorell Causeway bridge in order to obtain data on the residual bearing capacity. The load tests were carried out by applying two-point loads at third points of each beam. The presence of corrosion greatly reduced structural capacity, type of failure and the ductility of the beams compared to that classified with good external condition. Huffman[10] performed a full-scale load test of a bridge deck to investigate the load transfer between girders with varying degrees of damage. The bridge was built in 1967 in Ohio and replaced after 43 years of service. The bridge deck consisted of nine adjacent box beams collaborating through tie rods and shear keys. The aim was to observe structural residual capacity of beams with and without induced damage. The test was performed on site using steel frames and a three-point loading system. Osborn et al.[11] investigated the structural performance of seven PC bridge I-girders after being in service for 42 years in order to measure residual prestressing and shear resistance and compare it with AASHTO specifications. A group of five girders were tested in a three-point bending test configuration whereas two beams were subjected to shear capacity tests. Rogers et al.[12] performed 19 tests on pretensioned concrete bridge girders, 18 m span, with corroded reinforcement. Four-point loading tests up to failure were performed under load control and monotonic protocol to study the residual capacity, failure mode and consistency of the methodology to assess the capacity based on initial non-destructive survey. Barr et al.[13] analyzed the structural behavior of four I-girders. The specimens were used during expansion works of the original deck to accommodate additional lanes and were tested after being in service for 7 years. After estimating the prestressing loss, the girders were tested up to failure with a point load at different locations to investigate shear, flexure-shear, and flexure failures. Each of the tests showed a similar failure with concrete crushing in the slab, except for one specimen which failed with shear cracks leading from the support to the load and sliding of the prestressing strands. The tests confirmed that the AASHTO provisions on losses also on high strength concrete. Guiglia and

Taliano[14] performed an experimental campaign to test nine 40-year-old PC box girders with 35 m span and characterized by different state of deterioration. Rheological properties of concrete and residual prestressing were analyzed in loading the girders in service conditions. The girders were also tested up to failure under four-point bending configuration after two or three loading cycles. The most severely corroded specimens exhibited the tensile steel failure or shear-failure along the connection between the web and the bottom flange whereas two with localized corrosion exhibited failure of reinforcement and the remaining crushing of concrete top slab. Liu et al.[15] carried out load tests on four PC hollow beams that had been in service for 20 years in a freeze–thaw environment in China. The loading tests were performed in a four-point bending test configuration with distance between the two loading points of 2.0 and 5.2 m for each pair of beams and were aimed to check the ultimate capacity of the girders. In the first loading configuration, failure was achieved by the concrete crushing at the top edge; in the other configuration, slippage of the prestressed reinforcement and subsequent shear-compression failure was observed. Jeon et al.[16] presented experimental data on two 45-year-old post-tensioned bridge I-girders. The bending test was carried out in a three-point bending configuration with a single actuator located at midspan. One girder was loaded until concrete crushing at the concrete slab and the other was tested with multiple load steps to study residual prestressing with cracking of concrete and cutting selected wires. Tonelli et al.[17] performed a loading test on a 50-year-old viaduct, an Italian motorway bridge built in 1968 and decommissioned in 2005 after the failure of a pier caused by a landslide. The viaduct had three simply supported spans with four 32.5 m long PC girders. One span was subjected to several loading phases and testing protocols for materials and residual prestressing in service; a stop criterion based on a maximum midspan deflection of 300 mm for ultimate loading phase was employed. Visible torsion was evident from the longitudinally deformed shape of each girder, probably due to load redistribution, curb, different crack propagation or stiffness variability. In De Domenico et al.[18] static and dynamic tests also enhanced by non-destructive tests on a 55-year-old bridge still in service are reported. Field-test results also supported by experimental findings on the material characterization are used to calibrate a finite element (FE) model of the bridge deck, which is subsequently adopted for structural safety assessment of the bridge deck at ultimate limit state (ULS).

In this context, with the aim of providing a contribution to address the complex challenges in the assessment, maintenance, and management of existing bridges, the BRIDGE|50 research project was launched in 2018.[19–21] The project was established with the primary objective to deepen the understanding of the structural behavior and performance of aging bridges gathering data working with both a large number of members to be tested and by material testing procedures. The central focus of the experimental program is to investigate the structural performance of decommissioned bridge girders by conducting full-scale loading tests on various girder typologies, different degrees of deterioration, and distinct loading test configurations. These tests offer insights into the actual behavior of these structures, allowing the calibration of assessment models, the incorporation of uncertainties representative of actual bridge conditions, and the enhancement of statistical information essential for strength assessments. The structural members were retrieved from the Corso Grosseto viaduct, a 50-year-old viaduct located in Turin, Italy. This viaduct was the optimal mobility solution in an expanding area of the city.[22] Following the demolition, a total of 31 structural members, including 25 I-girders, 4 box girders, and 2 pier caps, were carefully removed and relocated in a wide testing site, where a series of non-destructive tests, destructive tests, and full-scale loading tests were conducted.[23] The initial phase of the loading test protocol focused on the evaluation of four girders, tested up to failure under a three-point bending configuration. This investigation encompassed concrete girders with both cast in situ slab and precast beam classified as undamaged.[22–27] This paper details a second phase of the loading test protocol, with the study of five I-girders subjected to a four-point bending configuration under service load and up to failure. Three different classes of damage were analyzed: undamaged state, damaged by dismantling operations and finally induced damage. The structural response was investigated considering several structural response indicators measured by a large system of sensors.

2 | DISMANTLED VIADUCT AND EXPERIMENTAL CAMPAIGN

2.1 | Corso Grosseto viaduct

The Corso Grosseto viaduct, built in Turin (Italy) in 1970, was a multilevel road bridge constructed to address the high traffic demand resulting from the rapid expansion of Italian industry and the subsequent population growth in northern Italy during that period. This structure consisted of 80 simply supported spans, ranging from 16 to 24 m and extending over a total length of about 1.4 km (Figure 1).

Each bridge deck consisted of 10 PC I-beams and two edges box beams, all interconnected by a top 140 mm thick cast-in situ concrete slab (Figure 2a). Additionally, two transverse beams were cast at third points along each span. According to the design documentation, the girders were prestressed using 17 straight strands along the bottom flange, distributed across two rows, and three strands on the top flange, each with a nominal diameter of 12.7 mm (Figure 2b). Five strands along the bottom flange, three spanning up to 5 m and two up to 3 m at the ends, were left unbonded using ducts. The box girders were designed to be roughly twice as resistant as the I-girders, by doubling the cross-section and the number of strands. The shear reinforcement consisted of ∅8 mm stirrups spaced at 170 mm for the first 1.3 m of the girder and 250 mm on average for the remaining part. The stirrups were also used to connect the precast beam with the cast-in situ concrete slab. Figure 2 shows a cross-section of the deck and technical drawings of both the I and box girders.

The piers were T-shaped and reached a maximum height of 12.4 m. The pier caps were post-tensioned using multiple groups of smooth wires along a curved profile. A group of tendons was released before placing the beams, and secondary prestressing was introduced before applying non-structural loads. Design documents indicated an ultimate tensile strength of prestressing steel of 1638 MPa and tension at 1% deformation 1474 MPa and a minimum requested cubic concrete compressive strength of 30 MPa at 28 days. Test reports issued in the 1970s by the Testing Laboratory of the Politecnico di Torino reported an average yielding and ultimate steel prestressing strength of 1486 and 1722 MPa, respectively, and a mean concrete compressive strength recorded at 28 days of 50.3 MPa over 4 samples and 40.5 MPa over 7 samples for precast I-beams and cast-in situ slab, respectively.[23] The maximum allowable stress for the strands immediately after tensioning was 1400 MPa. The total prestress loss was estimated at 40% of the initial stress after tensioning during the design stage. The girders were prestressed after steam curing with a 24-h operating cycle in the casting plant. The viaduct experienced exposure to aggressive atmospheric agents and large quantities of deicing salts, leading to evident problems of durability and multiple maintenance operations. In July 2017, deconstruction works started as part of a new urban redevelopment project commissioned by the Piedmont Region.

FIGURE 1 A view of the multilevel Corso Grosseto viaduct.

2.2 | The BRIDGE|50 research project

This project, established through a research agreement involving Politecnico di Milano, Politecnico di Torino, and several public authorities and private companies, investigates the residual structural performance of the structural elements of the viaduct.[19,20] More details can be found in Savino et al.[21–23] Figure 3 shows a detail of the structural members that were retrieved for investigation in their original configuration. The elements recovered for the research project to be tested are marked in green. The first set of elements tested under three-point

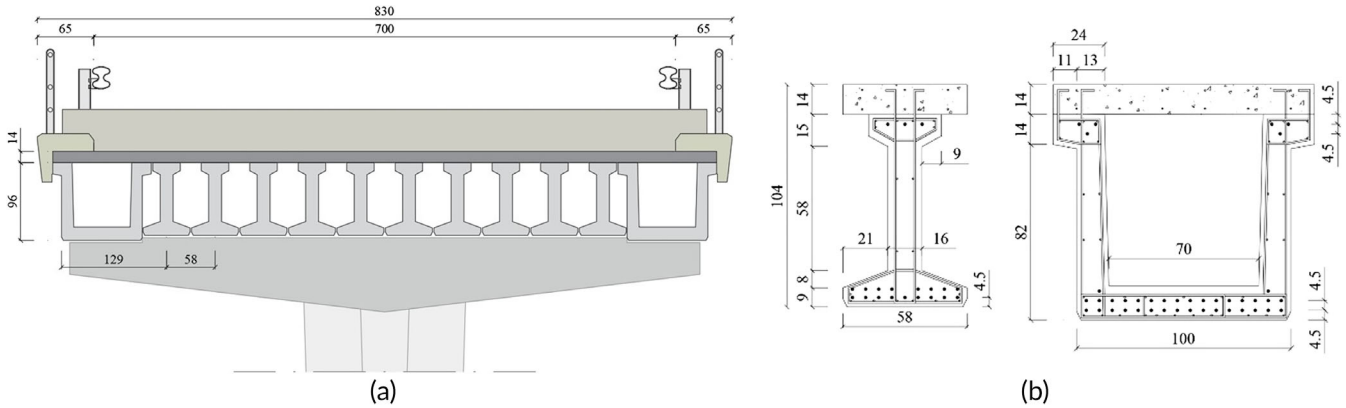

FIGURE 2 Cross-sections of (a) whole deck and (b) PC girders (cm).

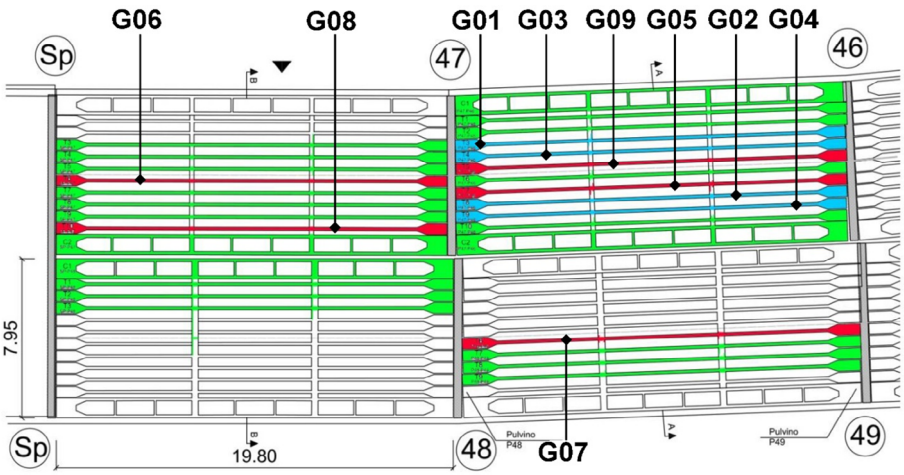

FIGURE 3 Top plan view of two adjacent spans of the in-service bridge deck with indication of the investigated deck girders. In red, the girders examined in this work. The numbering of the girders and their deck position is reported in Table 1.

TABLE 1 Tested deck beams and load protocols.

Girder ID	Deck code	Element type	Element state	Point loads	No. of loading phases
Tests reported in Savino et al.[23]					
G01	B3-P47/P46	I-beam with slab	Undamaged	3	2
G02	B8-P47/P46	I-beam with slab	Undamaged	3	2
G03	B4-P47/P46	I-beam with slab	Undamaged	3	1
G04	B9-P47/P46	I-beam	Undamaged	3	2
Tests reported in this paper					
G05	B7-P47/P46	I-beam with slab	Undamaged	4	2
G06	B6-Ab/P47	I-beam with slab	Undamaged	4	2
G07	B6-P48/P49	I-beam with slab	Damaged by dismantling	4	2
G08	B10-Ab/P47	I-beam with slab	Damaged by dismantling	4	2
G09	B5-P46/P47	I-beam with slab	Controlled damage	4	2

bending configurations are colored blue whereas the elements tested under four-point bending configurations, whose results are detailed in this paper, are highlighted in red. All elements were identified with a code[23] that corresponds to their original position in the bridge deck where the first two digits refer to the position of the girder on the deck (with respect to the coordinate system in Figure 1), and the following refer to "P" for Piers followed by its number and "Ab" stands for abutment. This paper reports the results for girders also with a more simple code such as for girder B7-P47/P46 it has been associated code G05 as detailed in Table 1. The span of all the girders was 19.2 m.

2.3 | Experimental program

The first phase of the project encompassed a series of preliminary activities, carried out prior to the dismantling of the viaduct, aimed to gain an initial understanding of its structural conditions. These activities included visual inspections in accordance with both national and international standards,[27] concrete coring and carbonation tests and sampling of reinforcing bars on the bridge piers. Subsequently, dynamic tests were performed on the four spans reported in Figure 3 before the dismantling process to characterize the overall dynamic behavior of the viaduct decks in their in-service configuration.[28] Once the structural elements were stored to the testing site, their condition was assessed using diagnostic techniques, including geometrical surveys, photographic relief, deterioration mapping, and electrochemical measurements to determine half-cell potentials, concrete electrical resistivity, and corrosion rate.[29–32] Further, rebound hammer tests and ultrasonic tests were conducted as an initial assessment of concrete strength to be compared with subsequent destructive test results.[33,34] The next phase involved the execution of full-scale loading tests

complemented by dynamic tests at both the undamaged stage and the subsequent post-cracking stage, aiming to establish correlations between the principal modal components and the corresponding level of damage induced by the applied load.[35–37] The final phase entailed a series of destructive tests for prestress loss assessment and mechanical characterization of materials.

Based on the findings from non-destructive surveys, four different categories were defined to distinguish undamaged elements, elements exhibiting corrosion damage, elements with damage resulting from dismantling operations, and those with controlled intentional damage. Based on these four categories, an appropriate loading test protocol was planned. In Savino et al.[23] the first four tests performed on undamaged girders under a three-point bending configuration are reported (Table 1). In the present paper, the results of the next five tests on girders with a four-point bending setup (in Table 1 from G05 to G09) are reported.

In Table 1, the deck code for each girder is listed to identify the original location on the deck (Figure 3). Girders G05 and G06 were classified as undamaged and were used as a reference to compare the load-carrying capacity of the other damaged girders. Girder G07 had two outermost strands cut during dismantling on either side of the lower flange at distances 3.7 m, 9.6 m (Figure 4a), and 15.4 m from the end section; the same girder has damage due to drilling operations at the same locations of the strands that, at midspan reduces the width of the cast in situ slab of 15 cm. For G08, two strands were cut just on one side at distances of 3.8 and 15.5 m, respectively (Figure 4b). Accordingly, both girders were classified as damaged by dismantling operations. Lastly, to explore the changes in flexural behavior comparable to a high level of damage due to corrosion or to that caused by an impact, a reduction of approximately 50% of the prestressing reinforcement was applied cutting a total of eight strands in the bottom flange; each strand was cut in two positions located 60 cm across the midspan, as shown in Figure 4c.

Each girder was tested under four-point bending configuration, with loads applied at a shear span of 6.5 m to ensure a wide constant bending moment zone.

2.4 | Material properties

After the loading tests, a further testing campaign was planned to evaluate the concrete properties and steel using direct destructive methods. The location of the specimens was selected in areas that experienced minimal stress during the loading protocols and showed no evidence of damage; they were retrieved from the first girders tested in Savino et al.[23] A total of 23 concrete core samples were extracted from the I-girders and 6 from the concrete slab, all intended for subsequent uniaxial compressive tests. The coring direction was horizontal in the longitudinal and transversal direction of the girder axis for slab and PC beam respectively, and the sample diameter was 74 mm to obtain a 2 to 1 ratio between length and diameter. To determine the tensile strength of the concrete, an additional 15 cores were extracted and subjected to tensile splitting strength tests. Samples of strands and rebars were retrieved from the ends of the girders that experienced only elastic stresses during the tests. Ten ordinary rebars with an 8 mm diameter and a length of 500 mm were collected for tensile testing. Besides, 19 strand samples with a length of

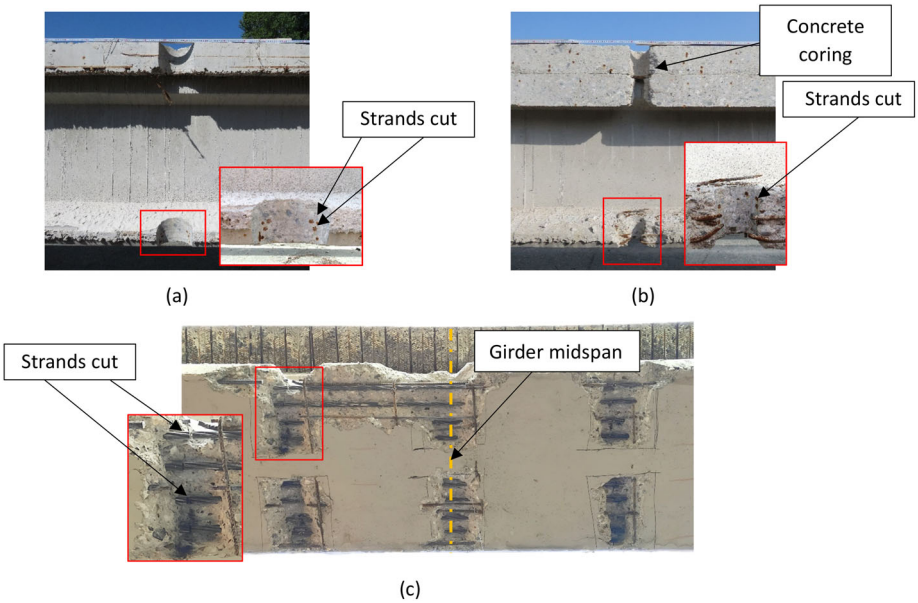

FIGURE 4 Damage detail for girders: (a) G07 lateral view, (b) G08 lateral view, and (c) G09 bottom view.

1200 mm were sampled for the mechanical properties of prestressing steel. The rebar samples were obtained from girders G01 and G05, while the prestressing steel samples were collected from girders B01, B03, B04, and B05. Table 2 summarizes the results of the destructive tests conducted according to European Standards with the mean values, standard deviations, and coefficients of variation (COV).

3 | LOADING TEST SETUP

The loading tests were conducted using a steel reaction frame provided by the Interdepartmental Center SISCON of Politecnico di Torino (Figure 5, www.siscon.polito.it). The equipment allows performing large scale tests on real structural members with a total load capacity of 4800 kN applicable in load controlled rate through two loading points with 750 mm of maximum stroke. More details on the facility are reported in Savino et al.[23]

The layout of the devices system has been designed to measure key parameters, providing multiple insights of the structural behavior. Table 3 provides a list of the measurement devices, which consists of 58 sensors for measuring strains, displacements, accelerations, and forces. The detailed layout of the instrumentation installed for each load test is shown in Figure 6. This paper only presents the outcomes of the devices for displacements, strains, and forces.

The shape of the girder due to deflection was recorded using three draw-wire sensors and six linear displacement transducers connected to the bottom side of the girders with Invar alloy wires. Linear displacement transducers were employed and installed on fixed frames to measure horizontal and vertical displacements at support zones. The relative slipping between strands and concrete was monitored by measuring relative displacements with respect to the girder edge face through linear displacement transducers.

TABLE 2 Material properties based on laboratory tests.

Material	Property	Unit	Mean value	Standard deviation	COV (%)
Concrete slab	Compressive strength	MPa	27.4	0.9	3.4
	Young's modulus	GPa	20.3	4.6	24.4
PC beam	Compressive strength	MPa	31.5	4.4	13.9
	Young's modulus	GPa	24.9	2.9	12.5
	Tensile strength	MPa	3.5	0.5	15.0
Prestressing steel	Yield's strength	MPa	1540.8	51.8	3.4
	Ultimate tensile strength	MPa	1786.9	44.3	3.1
	Young's modulus	GPa	201.1	8.9	4.4
Ordinary Rebar	Yield strength	MPa	449.0	24.2	5.4
	Ultimate tensile strength	MPa	685.1	41.0	6.0

FIGURE 5 Steel reaction frame with a deck beam in a four-point bending test configuration.

TABLE 3 Sensor layout for a four-point bending test setup (Figure 6).

Parameter	Sensor	Location	Number
Deflection	Potentiometer displacement transducer	D01–D09, V01, V02, H01	12
Strand sliding	Potentiometer displacement transducer	STR01, STR02	2
Slab sliding	Potentiometer displacement transducer	Sl	1
Shear strain	Linear variable displacement Transducer (LVDT)	SH1A/B-SH8A/B	16
Bending strain	Linear variable displacement Transducer (LVDT)	B01T-B06T B01C-B06C	12
Bending strain	Electric Strain gauge	SG1-SG2	2
Acceleration	Accelerometer	1Z-10Z and 10Y	10
Load	Load cell	Hydraulic jacks	3

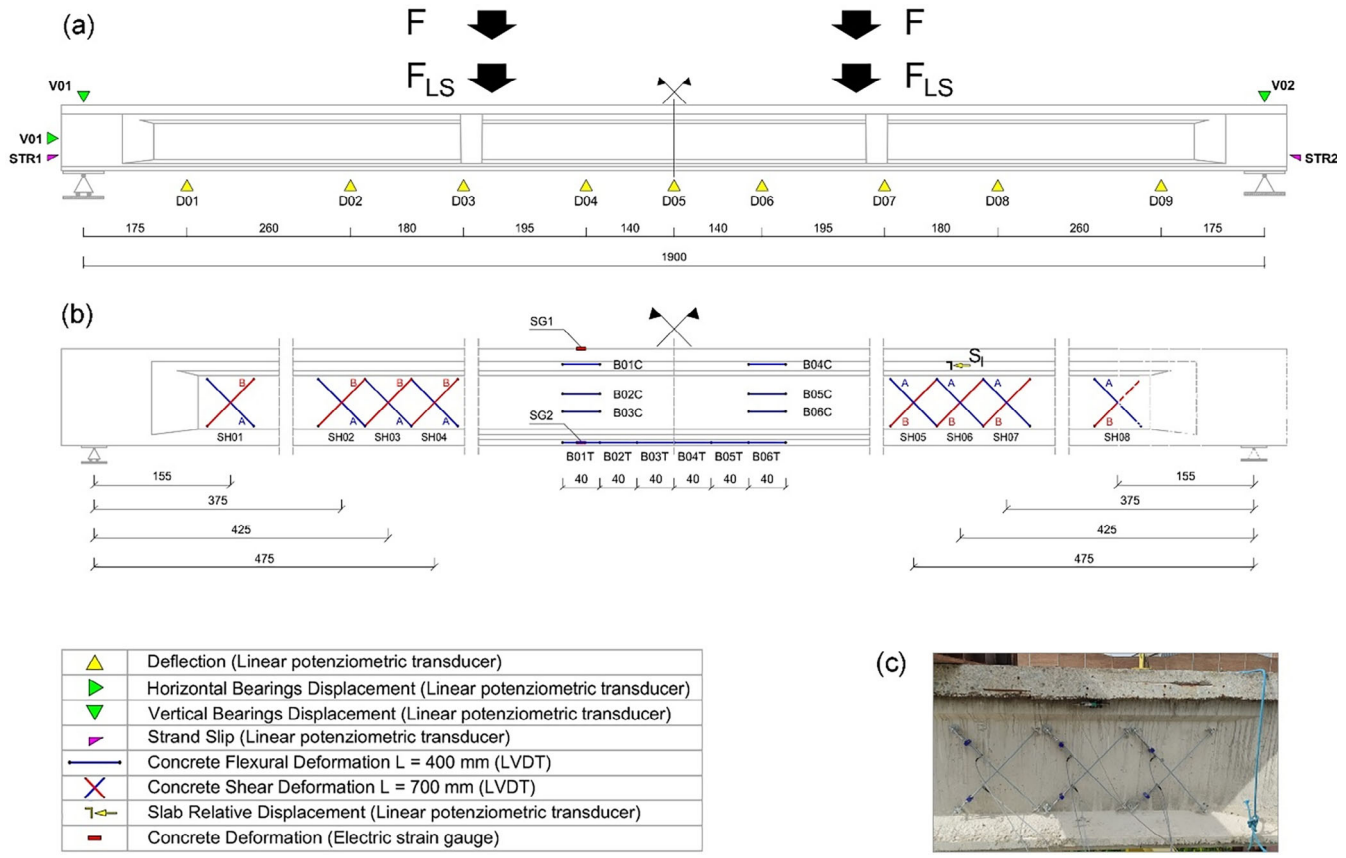

FIGURE 6 Four-point bending test setup and layout of the measurement system (cm) with detail of LVDT on supporting frame.

The strain and the opening of the concrete cracks induced by flexural stresses were measured using LVDTs mounted on a 400-mm base (Figure 6). The estimation of the deformation along a transversal section near the mid-span of the beam was completed by applying two electrical 120 Ohm, 20 mm length strain gauges installed on the cast in situ concrete slab and on the bottom flange of the PC beam.

Concrete shear strains were evaluated along the shear spans using LVDTs installed on supporting frames oriented at a 45° angle and a measurement base of 700 mm. The applied load was measured with load cells placed between the actuators and the thrust block to measure the forces acting on the girder and ensure symmetrical loading condition (Figure 6).

The test protocol was designed with an initial loading phase to achieve stabilized crack openings, followed by a second loading phase up to failure. The two phases were meant for the determination of both cracking and decompression load.

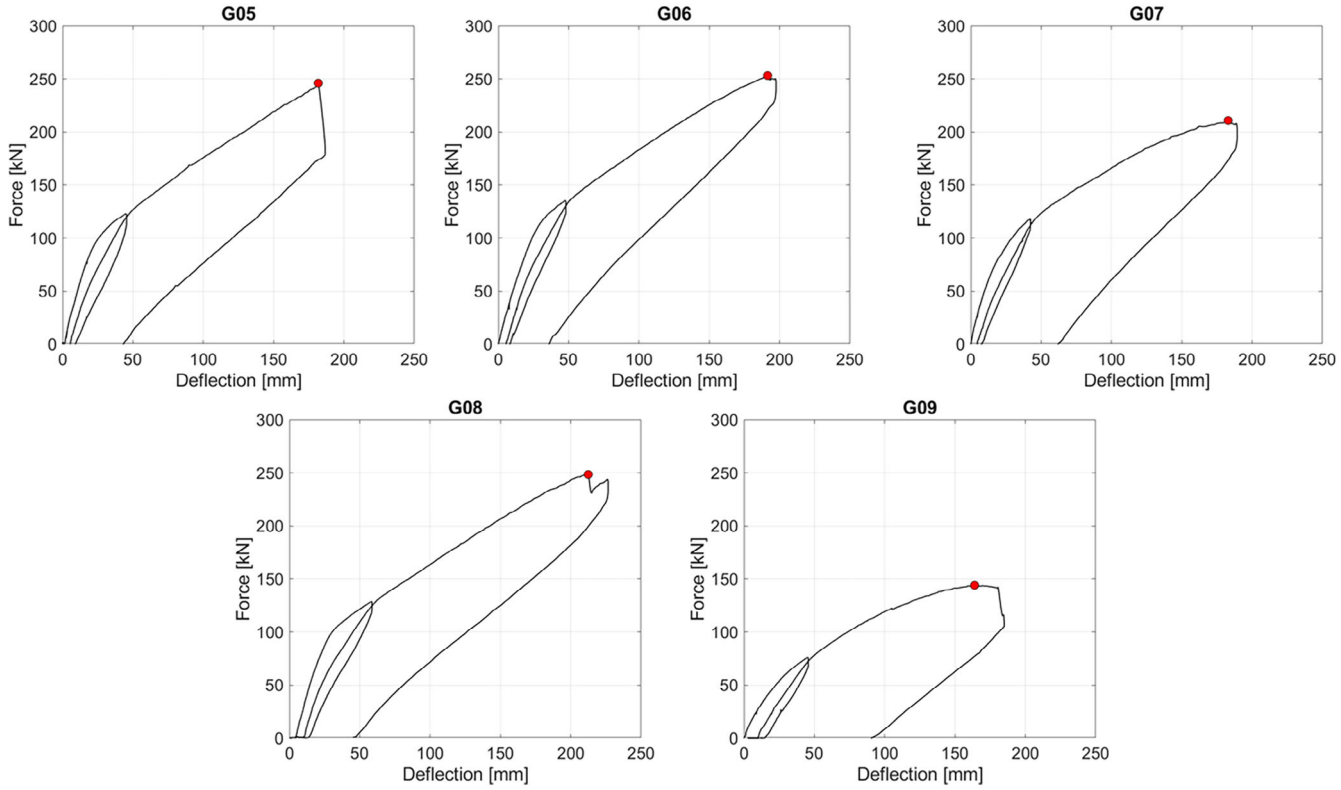

FIGURE 7 Load F-midspan deflection diagrams of the tested girders (Table 1).

4 | EXPERIMENTAL RESULTS

This paper presents the most significant outcomes of the recorded parameters that describe the structural response of the girders, designated G05, G06, G07, G08, and G09, that were tested under static loading procedure at different rates: 6.0, 7.5, 4.8, 4.5, and 2.4 kN/min, respectively. All the loading rates used for the tests ensured a quasi-static loading path; nevertheless, the differences among the tests are attributable to the estimated total time required to complete the test and on-field operative conditions, being the activities made outdoor.

In the following, the indicated load F corresponds to the force transmitted by one of the loading points (according to "F" reported in Figure 6). The total load applied to the girder was calculated by adding the weight of the loading system F_{LS} (reported in Figure 6 and estimated at 23.64 kN for each loading point) to the recorded applied load.

4.1 | Global structural response

The curves load-deflection at the midspan (position D05 as in Figure 6) of the five girders are reported in Figure 7. During the first loading phase, the load-deflection response followed a linear trend, highlighting the elastic behavior of the tested beams. As the load level approached the stabilized cracking stage, the rate of deflection increased due to a progressive stiffness reduction. The descending branch revealed a residual deflection of less than 10 mm. The reloading branch had a slope almost parallel to the first and an anticipated nonlinear deviation up to the maximum load level reached at the first cycle. It is worth noting that the initial stiffness of girder G09 was lower compared to the other girders

TABLE 4 Total load (2F) at failure and corresponding midspan deflection.

Girder	F_{max} (kN)	$\delta_{midspan}$ (mm)
Tests reported in Savino et al.[23]		
G01	313.0	178.92
G02	338.2	151.24
G03	288.6	148.16
G04	258.2	145.06
Tests reported in this paper		
G05	480.4	179.9
G06	506.0	191.3
G07	422.4	184.3
G08	496.0	205.5
G09	289.6	163.4

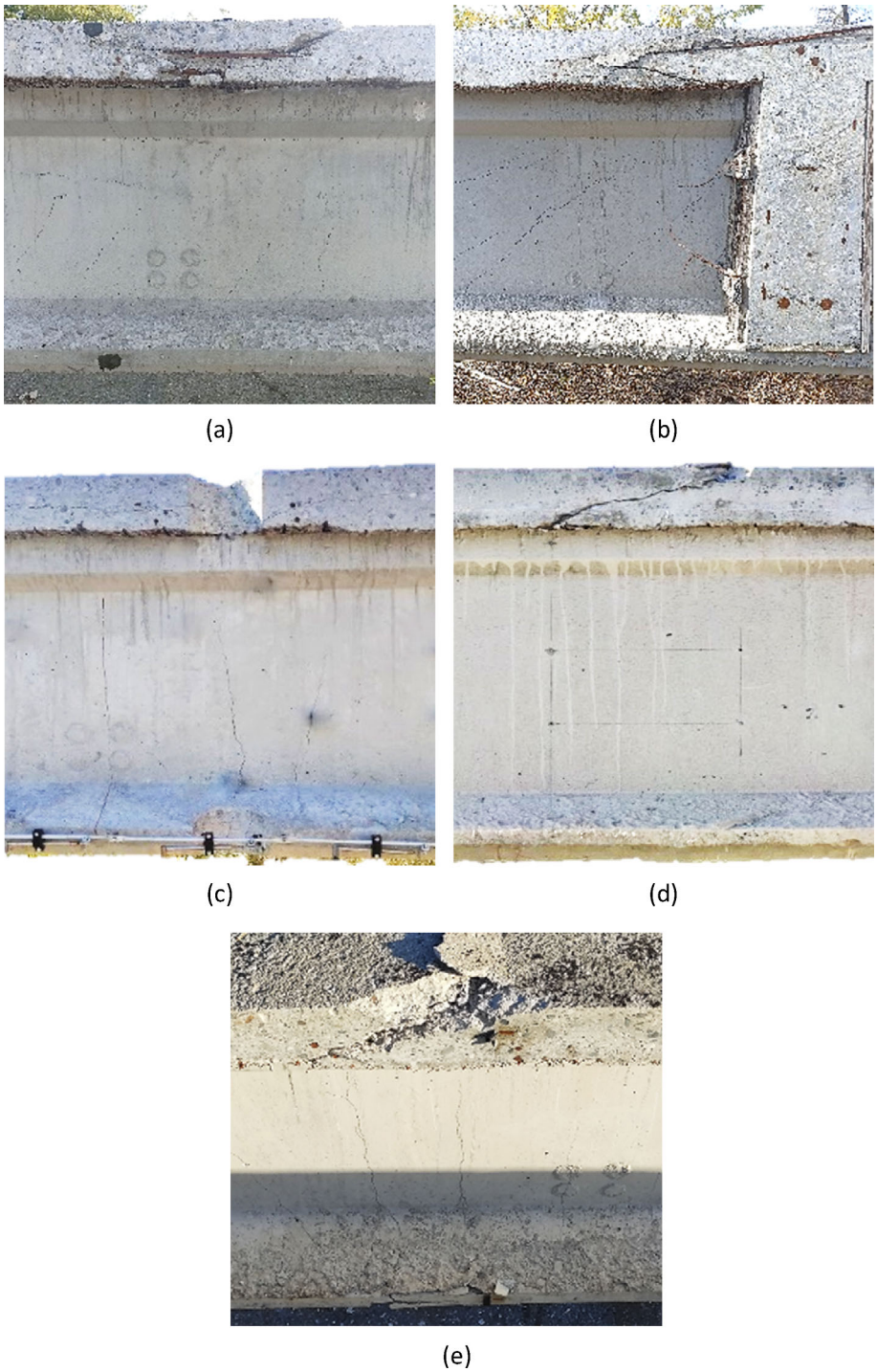

FIGURE 8 Detail of the failure zones of the tested girders (Table 1): (a) G05, (b) G06, (c) G07, (d) G08, and (e) G09.

and the transition from the elastic to the cracked phase was smoother.

Each girder failed by crushing of the cast-in situ concrete slab; a similar behavior was registered with the three-point bending tests.[23] In Table 4, the total load applied and the corresponding midspan deflections for the girders, also considering the tests reported in Savino et all.[23] are reported. The rupture, pictured in Figure 8, occurred in all girders in the region between the two loading points, with the exception of girder G06 which failed close to a load point but along the shear span.

Figure 9 shows the deflection profiles recorded at different load levels for each girder, covering both the elastic and post-cracking phases. These deflection measurements were taken at sensor positions from D01 to D09 according to the layout of Figure 6. Girders G05 and G06 exhibited similar deflections due to their sound conservation state as undamaged girders. Accordingly, G07 and G08, having similar damages, showed progressively

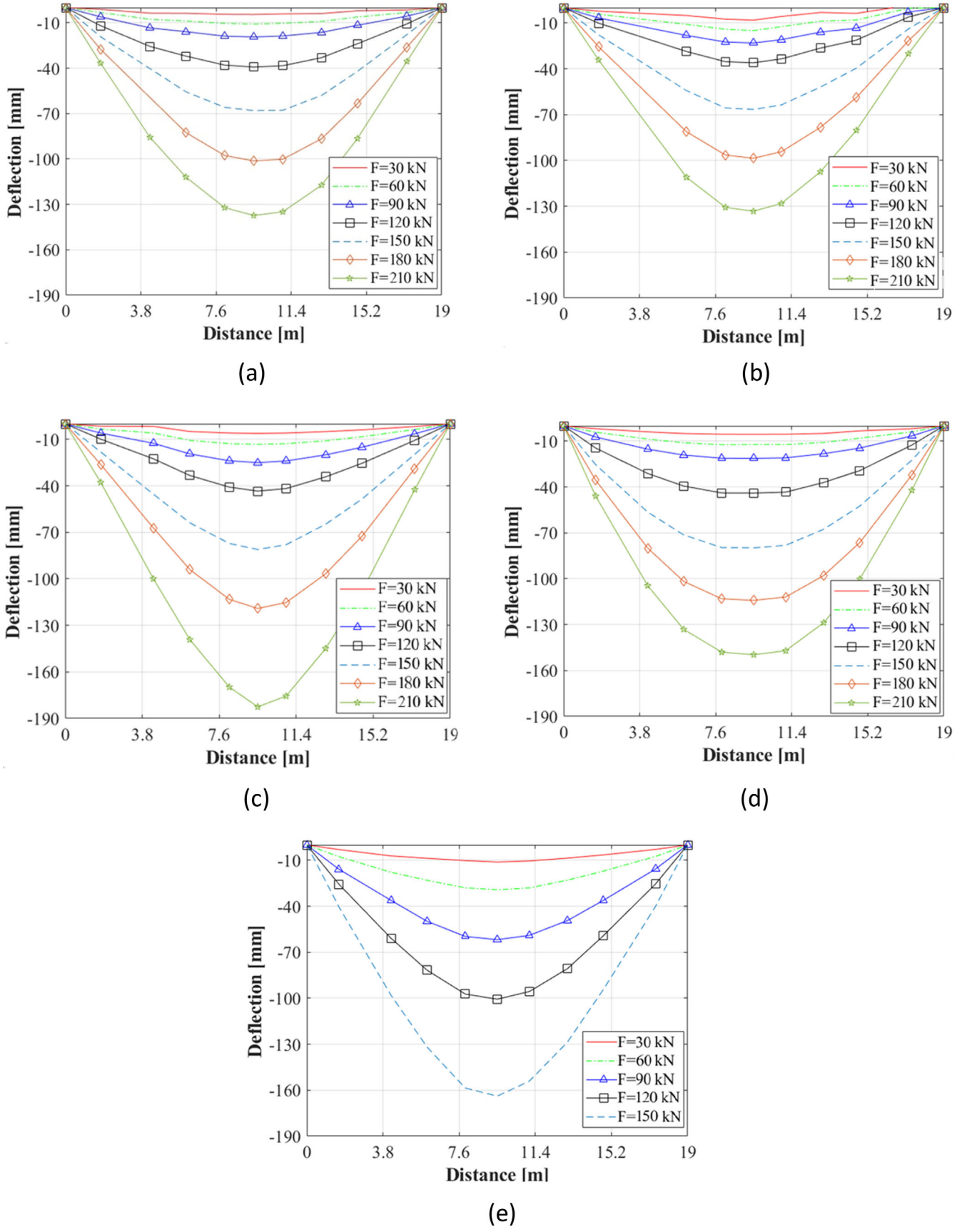

FIGURE 9 Deflection shape of the tested girders (Table 1): (a) G05, (b) G06, (c) G07, (d) G08, and (e) G09.

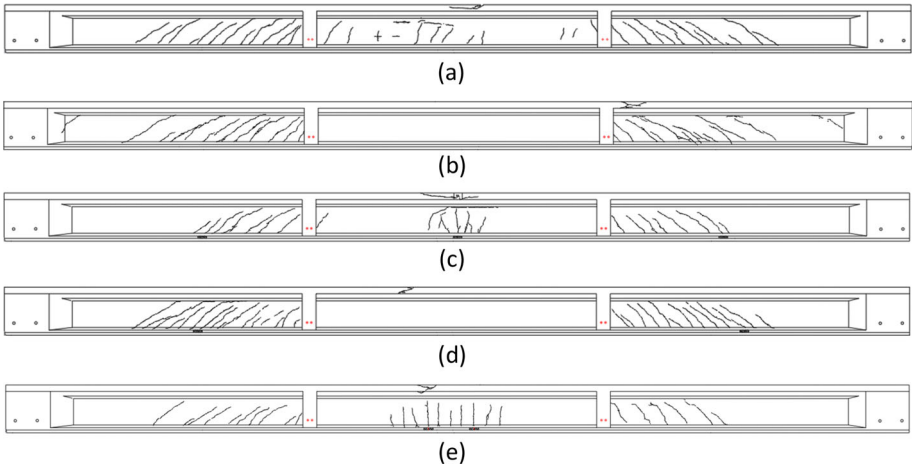

FIGURE 10 Crack pattern of the tested girders after failure (Table 1): (a) G05, (b) G06, (c) G07, (d) G08, and (e) G09.

higher deflections compared to the undamaged girders, and the differences became more pronounced at higher load levels. Girder G09, intentionally damaged, exhibited the largest deflections at the same load levels compared to the other girders due to an impaired flexural stiffness.

The residual crack patterns recorded after the loading tests on the girders are reported in Figure 10. All the girders show an evident residual crack pattern attributable to shear effect; they are characterized by the inclination and their presence outside the constant moment region. The shear cracks remained visible after testing probably because of a larger interlock effect than the flexural cracks that tend to completely close because of prestressing still effective after the load removal.

For girder G09 with a reduced number of prestressing strands across at midspan, vertical cracks in the central part of it due to bending were still highly visible in this region. For the first four girders, the residual crack evidenced outside the constant moment region, and it extended diagonally from the bottom flange to the top flange of the PC girder.

4.2 | First cracking and decompression load

The first cracking and decompression loads are the parameters usually adopted to estimate the residual prestressing in experimental testing of prestressed concrete elements.

In this work, the procedure adopted involved the analysis of the mean tensile deformation in the bottom chords measured by LVDT sensors BT in Figure 6, which covers a 2.4 m length across the midspan and can be assumed as representative of the average strain on the tensile zone.[14]

Cracking and decompression load estimates are obtained by identifying the change in slope of the secant stiffness as the ratio between forces applied and relative average measured strains (see Formula 1). For each test, the reference force level (F_{ref} and corresponding strain ε_{ref}) is chosen to be greater than a minimum load at which the four actuators start to push on the loading system.

$$\Delta K_i = (F_i - F_{ref})/(\varepsilon_i - \varepsilon_{ref}) \quad (1)$$

During the first phase of the test, the stress in the bottom fiber increases proportionally to the external load imposed by the actuators until the concrete bottom fiber reaches the tensile strength. At higher load levels, the mean deformation rate in the tensile zone varies sharply, being directly influenced by the rise in the neutral axis over the section due to cracks opening up. For uncracked girders, the variation in slope corresponds to the reaching of the cracking moment. On the other hand, for an element that is already cracked, such as the girders in the second load stage, the sharp variation in secant stiffness indicates that the residual prestressing load has been overcome. It is worth noticing that in girder G09 the values of cracking and decompression loads estimated in the two loading phases coincide (Table 5 and Figure 11).

TABLE 5 Cracking and decompression loads.

Girder	Cracking load (F) (kN)	Decompression load (F) (kN)
G05	55.4	38.8
G06	58.4	40.5
G07	35.4	30.4
G08	48.0	37.8
G09	29.6	29.4

4.3 | Measured strains in concrete

As all the girders failed due to crushing of the concrete slab, the compressive strain recorded in the upper region of the girders is a critical parameter for examining their

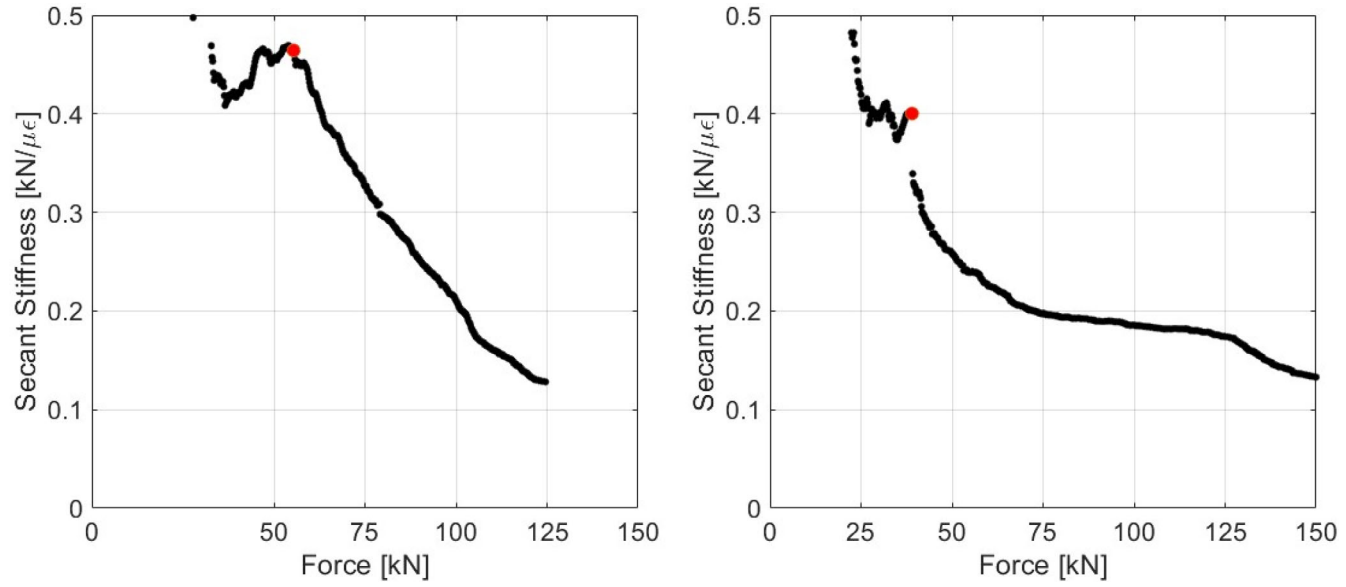

FIGURE 11 Secant stiffness vs. force diagram, calculated from the mean tensile deformation measured by BT transducers in the bottom flange of the girder. The red dots indicate the opening of the cracks (left figure) and the decompression load (right).

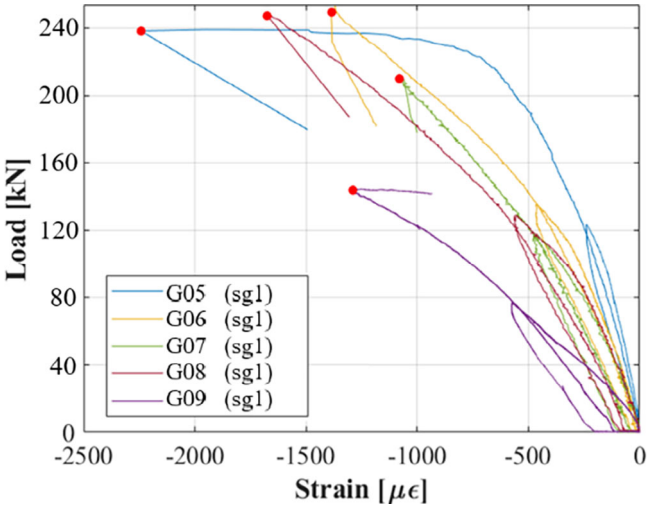

FIGURE 12 Load-compressive strain diagrams of the tested girders (Table 1): G05, G06, G07, G08, and G09.

structural response during the load test. Figure 12 shows the selected compressive strain curves of the cast-in situ slab in the tested beams. For girders without prior damage, a linear increase in concrete strain is observed prior to cracking. Once the load exceeds the cracking point, the strain increases, evidencing the non-linear behavior. The strain gauge for the G05 girder was found to be very close to the crushed zone, giving an ultimate compressive strain of −2242 με. However, for girders G06, G07, G08, and G09, the strain gauge was positioned away from the crushing zone; the maximum compressive strains recorded were −1385 με, −1080 με, −1675 με, and −1290 με, respectively.

Bending and shear mechanisms were observed through LVDTs with the schemes reported in Figure 6. As an illustrative case of shear behavior of both an undamaged girder and a girder subjected to induced damage, the diagonal strains recorded for G06 and G07 girders are shown in Figure 13. The curves are color coded according to the respective LVDT locations, and a distinct dotted line is used to distinguish between the left shear span (represented by dashed lines) and the right shear span (represented by continuous lines). At a load of approximately 120 kN on the girders, diagonal cracks were observed in the web along the shear span. However, as the maximum load was approached, different resistance mechanisms were activated in the two girders. In particular, the shear strains exhibited by G07 were lower than those of the undamaged girder, which is related to the reduced shear stress in this case. In both cases, prominent shear cracking was observed close to the loading points. It is worth noting that the four-point bending setup induced higher levels of shear strains than the previous three-point bending tests.[24]

The following Figure 14 shows the strain distribution along the cross section at various loads for the two previously selected girders. According to the graphs, the cross section of the girders before cracking basically complies with the hypothesis of plane section deformation at various load levels. At this stage, the ratio between the height of the compressive zone and the effective height of G06 and G07 girder was about 0.46 and 0.52, respectively. When cracking occurred, the neutral axis moved up the cross section and the strain distribution is not planar anymore. Outcomes from measuring devices in the tension

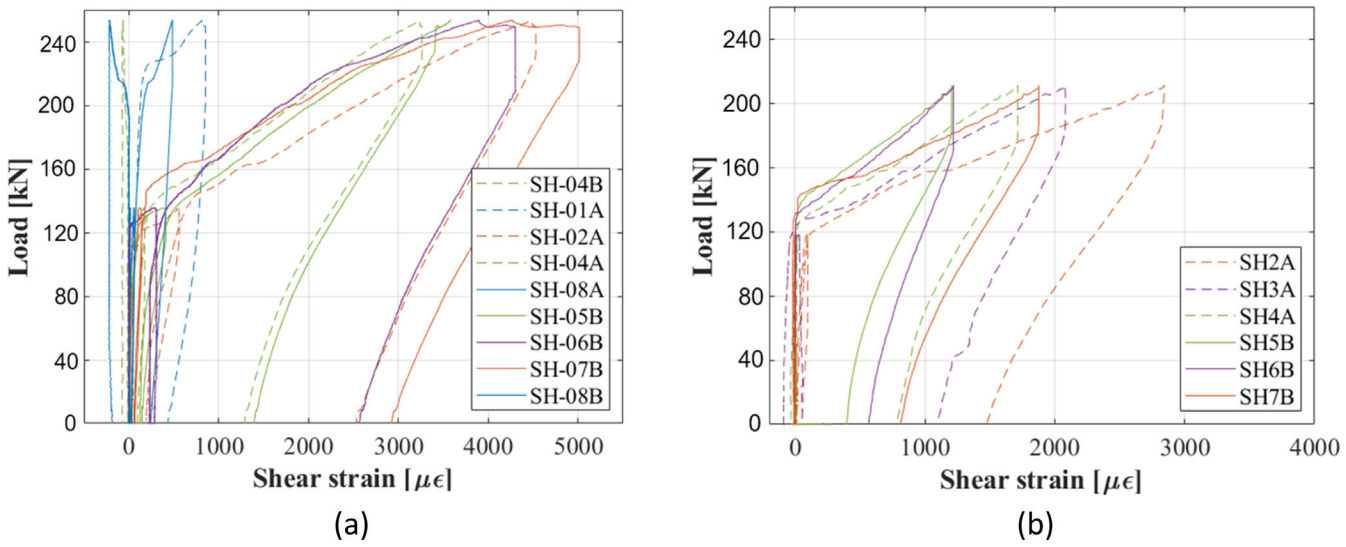

FIGURE 13 Load-shear strain diagrams of the tested girders (Table 1): (a) G06 and (b) G07.

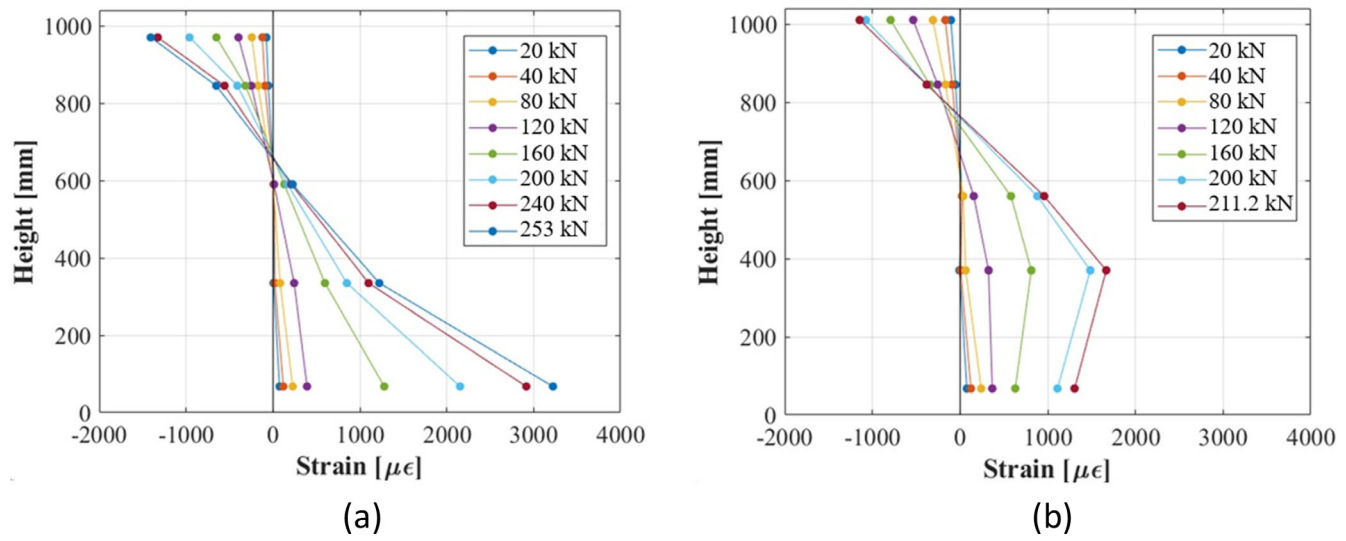

FIGURE 14 Cross-section strain (recorded by sg1, C-01, C-02, C-03, and T-01) of the tested girders (Table 1): (a) G06 and (b) G07.

zone, being attached to the concrete, should be used with caution because they could be affected by cracking. When the applied load reached the ultimate value, the aforementioned ratio decreased to 0.30 and 0.27, respectively.

5 | DISCUSSION

In Figure 7, the tested girders exhibited a typical trend in their load-deflection response, characterized by an initial substantially linear elastic phase, followed by a nonlinear response after flexural cracking. As the applied load increases, concrete cracking becomes more pronounced in the pure bending region, resulting in an upward shift of the position of the neutral axis (Figure 14). During reloading, a relatively smooth transition was observed due to the further progressive rise of the neutral axis on the cross-section in the cracked state. The G09 girder with induced damage across the midspan shows the effect of the damage with a smoother transition to the cracked stage compared to the other girders. Moreover, a global lower flexural stiffness was registered comparing the whole load-deflection curve with the undamaged ones. Residual deflection after the first loading cycle can be observed due to non-recoverable deformation caused by cracking; for specimen G09, residual deflection was almost double compared to the other girders due to the larger nonlinearities enhanced by flexural cracking.

TABLE 6 Total cracking load (2F) and initial uncracked flexural stiffness.

Girder	Total cracking load F_2 (kN)	$\overline{F}-F_1$ (kN)	$\delta-\delta_1$ (mm)	K_{EXP} (kN/m)	$K_{T\text{-}P}$ (kN/m)	$K_{T\text{-}EXP}$ (kN/m)
G01	90.8	35.4	4.82	7355	8516	6651
G02	70.8	25.4	3.35	7574		
G03	64.8	20.4	2.73	7472		
G04	74.8	27.3	7.11	3849	4405	3676
G05	100.0	20.1	1.68	11,927	9931	7722
G06	102.0	41.1	4.23	9709		
G07	102.4	39.8	4.14	9630		
G08	110.0	45.1	4.50	10,014		
G09	80.4	28.8	5.82	4945	6192	4854

The results also showed differences among the girders between the cracking loads and the decompression loads. Specifically, the cracking loads ranged from 29.6 to 58.4 kN and were found to be larger than the range 29.4–40.5 kN for decompression loads (Table 5). Therefore, it could be possible to state that the tested girders, with the exception of G09, have never reached that level of loading along their service life.

In order to evaluate the structural response in service conditions, a comparison among all the girders tested so far within the BRIDGE|50 research project together with an elastic numerical models is proposed in terms of initial uncracked flexural stiffness (UFS), considering the slope of secant line in the force – midspan deflection diagram between the points F_1 and $\overline{F}$, where:

F_1 is the total load applied of 20 kN;

$$\overline{F}=(F_1+F_2)/2$$

being F_2 as the total load at first cracking calculated on load–displacement curves with analogous approach as in Section 4.2:

$\overline{\delta}$ is the midspan deflection at load $\overline{F}$.

δ_1 is the midspan deflection at initial load F_1, $K_{EXP}=(\overline{F}-F_1)/(\overline{\delta}-\delta_1)$, $K_{T\text{-}P}$ and $K_{T\text{-}EXP}$ are the theoretical UFS obtained from a linear elastic finite element analysis using design and experimental mean values of elastic modulus of materials (Table 2), respectively. The FE model, built with solid elements is constituted by 1123 nodes and 681 solid 8-nodes elements. Boundary conditions and loading layout simulate the test setup. In Table 6 the results of this approach is reported.

Theoretical $K_{T\text{-}P}$ and $K_{T\text{-}EXP}$ are the same for the first three girders listed in the table whereas they are different for G04 due to the removal of the slab (tested under three point bending test). They are also the same for the rest of the girders (under four point bending test) except for G09 due to local damage induced by strand cut. In general, the measured stiffnesses K_{EXP} are quite close to the values obtained by numerical simulation using design values $K_{T\text{-}P}$, in particular for beam tested under four point bending configuration. Conversely, with the first four beams tested under three point bending configuration, larger values $K_{T\text{-}P}$ compared to K_{EXP} are recorded. The last column reporting $K_{T\text{-}EXP}$ evidences a general underestimation of UFS adopting the results of material testing as reported in Table 2. The systematic deviation of values obtained for $K_{T\text{-}EXP}$ may reflect local tests effect influenced by the coring disturbance during sampling. The effects of damage are evident in reducing the bending stiffness for G04 and G09. It is noteworthy that this procedure, being non-destructive, can be used for structures in service to estimate the level of damage through proof loading tests and then useful for structural monitoring.

In order to compare all the girders tested, in Table 7 some parameters at failure are reported including the outcomes of the tests described in Savino et al.[23] The parameter M_{EXP} is the experimental resisting moment of the girder evaluated in the rupture section that has been calculated by adding the moment capacity to the effect in terms of bending moment of the self-weight and the weight of the loading system. This allows one to directly match all the resistances of the girders disregarding their static schemes.

From Table 7, in terms of resistance in bending M_{EXP}, girders classified as undamaged (Table 1) can be considered as a reference. The mean value $M_{EXP,AV}$ of this group of girders is 1901.4 kNm with a maximum deviation of 6.5%. The absence of the cast in situ slab in girder G04 gives a 17.5% reduction with respect to M_{EXP}. The girder G07, with strands cut at midspan (equivalent to a 23.5% reduction in strands in the lower flange) and 15 cm of width of cast in situ slab missing due to drilling activity for lifting operations during dismantling, experiences a 3.4% reduction in strength. Girder G08 had the

TABLE 7 Parameters at failure.

Girder	Shear span (m)	Rupture location[a] (m)	M_{EXP} (kNm)	Element state (—)
G01	9.2	10.5	1838.8	Undamaged
G02	9.2	10.4	1965.8	Undamaged
G03	9.2	9.1	1838.7	Undamaged
G04	9.2	8.8	1568.2	Undamaged
G05	6.5	9.9	2025.5	Undamaged
G06	6.5	13.3	1838.2	Undamaged
G07	6.5	9.6	1837.5	Damaged by dismantling
G08	6.5	8.6	2074.0	Damaged by dismantling
G09	6.5	9.0	1405.1	Controlled damage

[a]Measured from left support.

highest M_{EXP} even though it was classified as damaged (see Section 2.3); the influence of the damage did not likely affect the capacity being localized out of the most stressed zones. Girder G09, with eight strands cut (equivalent to a 47.1% reduction in strands in the bottom flange), showed a 26.1% reduction in strength compared to $M_{EXP,AV}$. The design of the viaduct, completed in 1970, reports a design moment ($M_{S\text{-}70}$) based on allowable stress method of 823.9 kNm. Notable, the bending capacity of the most damaged girder (G09) tested after 50 years of service equal to 1405.1 kNm was still about 1.7 times the design moment $M_{S\text{-}70}$.

On the other hand, the structural resistance at ultimate limit state of the resistant bending moment $M_{R,NTC}$ is equal to 2201.2 kNm; this is calculated according to the current Italian Code (NTC2018[38]) and using the average values of resistances of materials for concrete and steel, coming from destructive tests (Table 2). This value overestimates by 16% the value $M_{EXP,AV}$ highlighting the significance of the present work. The same procedure applied to evaluate the structural resistance at ultimate limit state of the I beam without the cast in situ slab gives a $M_{R,NTC} = 1611.7$ kNm that is very similar to the bending resistance registered for girder G04 (variation of 2.8%, see Table 7). The differences can be attributed to the variability in strength characteristics of the cast in situ slab other than possible slip between that and the precast beam, even if the readings from the specific device report that none of the girders tested showed any relevant slip.

6 | CONCLUSIONS

The results of an investigation conducted as part of the BRIDGE|50 research project, focusing on large-scale loading tests performed on five 50-years-old PC girders, have been reported. The study encompassed an experimental campaign aimed at evaluating the structural response of five girders subjected to four-point bending tests at varying levels of deterioration with two primary deterioration scenarios: strand cutting during dismantling operations and intentional strand cutting at midspan before testing. The extent of damage had a valuable impact on the strength of the girders, with the most heavily damaged one still exhibiting a capacity of about 1.7 times the design bending moment (evaluated at the time of construction), despite a 47.1% reduction in strands at midspan. Each girder failed in a brittle manner, by compressive failure of the cast-in-situ concrete slab, but with varying cracking patterns related to the level of induced damage. A key role is played by the cast in situ slab that, with its limited Young's modulus affecting the service behavior and with its low resistance providing limited capacity. A destructive testing campaign was conducted after the loading tests which provided information about the quality and properties of the concrete and steel used in the tested girders. The experimental results, also compared with numerical results of finite element analysis, were elaborated to estimate the uncracked initial bending stiffness to be used for in service evaluation conditions. It can be noted that the finite element analysis, adopting the mechanical properties based on experimental tests, overestimates the deflection of the structure. Resisting moments at failure were obtained and compared with the results of previous investigations of the same authors[23] performed under different load schemes. The load carrying capacity of the girders estimated by using the model suggested by the Italian Code brings to a higher value of the experimental load resistance. The collected data contribute to build a database within the BRIDGE|50 research project activities for theoretical and numerical models fitting, and it enables reducing uncertainties in modeling.[39] Other activities will concern the execution of full-scale loading

tests with reduced shear span in order to analyze more in detail the shear resisting mechanisms.

ACKNOWLEDGMENTS

BRIDGE|50 is a research project based on a research agreement among universities, public authorities, and private companies. Members of the Management Committee: S.C.R. Piemonte S.p.A. (President); Politecnico di Milano (Scientific Coordinator); Politecnico di Torino (Scientific Responsible of the Experimental Activities); Lombardi Engineering (Secretary); Piedmont Region; City of Turin; Metropolitan City of Turin; TNE Torino Nuova Economia; ATI Itinera & C.M.B.; ATI Despe & Perino Piero; Quaranta Group. BRIDGE|50 website: https://www.bridge50.org.

DATA AVAILABILITY STATEMENT

The data that support the findings of this study are available from the corresponding author upon reasonable request.

ORCID

Francesco Tondolo https://orcid.org/0000-0003-0258-3054

Antonino Quattrone https://orcid.org/0000-0003-4856-051X

Fabio Biondini https://orcid.org/0000-0003-1142-6261

REFERENCES

1. Biondini F, Frangopol DM. Life-cycle performance of deteriorating structural systems under uncertainty: review. J Struct Eng ASCE. 2016;142(9):1–17.
2. Biondini F, Frangopol DM. Life-cycle design, assessment and maintenance of structures and infrastructure systems. Reston, VA, USA: American Society of Civil Engineers (ASCE); 2019.
3. Biondini F, Lounis Z, Ghosn M. Effects of climate change on life-cycle performance of structures and infrastructure systems: safety, reliability, and risk. Reston, VA: American Society of Civil Engineers (ASCE); 2024.
4. Shenoy CV, Frantz GC. Structural tests of 27-year-old prestressed concrete bridge beams. PCI J. 1991;36:80–90.
5. Azizinamini A, Keeler BJ, Rohde J, Mehrabi AB. Application of a new nondestructive evaluation technique to a 25-year-old prestressed concrete girder. PCI J. 1996;41:82–95.
6. Halsey T, Miller R. Destructive testing of two forty-year-old prestressed concrete bridge beams. PCI J. 1996;41:84–93.
7. Pessiki S, Kaczinski M, Wescott HH. Evaluation of effective prestress force in 28-year-old prestressed concrete bridge beams. PCI J. 1996;41:78–89.
8. Eder RW, Miller RA, Baseheart TM, Swanson JA. Testing of two 50-year-old precast post-tensioned concrete bridge girders. PCI J. 2005;50:90–5.
9. Pape TM, Melchers RE. The effects of corrosion on 45-year-old pre-stressed concrete bridge beams. Struct Infrastruct Eng. 2011;7(1–2):101–8.
10. Huffman JM. Destructive Testing of a Full-Scale 43 Year Old Adjacent Prestressed Concrete Box Beam Bridge: Middle and West Spans [Master's thesis, Ohio University]. 2012 OhioLINK Electronic Theses and Dissertations Center.
11. Osborn GP, Barr PJ, Petty DA, Halling MW, Brackus TR. Residual prestress forces and shear capacity of salvaged prestressed concrete bridge girders. J Bridge Eng. 2012;17:302–9.
12. Rogers RA, Wotherspoon L, Scott A, Ingham JM. Residual strength assessment and destructive testing of decommissioned concrete bridge beams with corroded pretensioned reinforcement. PCI J. 2012;57(3):100–18.
13. Barr P, Higgs A, Halling M. Forensic Testing of Prestress Concrete Girders after Forty Years of Service. Final Report. 2013.
14. Guiglia M, Taliano M. Experimental analysis of the effective pre-stress in large-span bridge box girders after 40 years of service life. Eng Struct. 2014;66:146–58.
15. Liu J, Jia Y. Destructive testing of twenty-year-old prestressed concrete bridge beams in freezing-thawing region. Civ Eng J. 2019;3:344–56.
16. Jeon CH, Sim C, Shim CS. The effect of wire rupture on flexural behaviour of 45-year-old post-tensioned concrete bridge girders. Eng Struct. 2021;245:112842.
17. Tonelli D, Rossi F, Brighenti F, Verzobio A, Bonelli A, Zonta D. Prestressed concrete bridge tested to failure: the Alveo Vecchio viaduct case study. J Civ Struct Health Monit. 2022;13:873–99.
18. De Domenico D, Messina D, Recupero A. Quality control and safety assessment of prestressed concrete bridge decks through combined field tests and numerical simulation. Structure. 2022;39:1135–57.
19. Biondini F, Manto S, Beltrami C, Tondolo F, Chiara M, Salza B, et al. BRIDGE|50 research project: residual structural performance of a 50-year-old bridge. 10th international conference on bridge maintenance, safety and management (IABMAS 2020), June 28–July 2, 2020 (postponed to April 11–15, 2021), Sapporo, Japan. In: Yokota H, Frangopol DM, editors. Bridge maintenance, safety, management, life-cycle sustainability and innovations. London, UK: CRC Press/Balkema, Taylor & Francis Group; 2020.
20. Biondini F, Tondolo F, Manto S, Beltrami C, Chiara M, Salza B, et al. Residual structural performance of existing PC bridges: recent advances of the BRIDGE|50 research project. 1st conference of the European association on quality control of bridges and structures (EUROSTRUCT 2021), Padua, Italy, august 29–September 1, 2021. In: Pellegrino C, Faleschini F, Zanini MA, Matos JC, Casas JR, Strauss A, editors. Lecture notes in civil engineering. Volume 200. Germany: Springer Germany: Science and Business Media; 2022.
21. Savino P, Anghileri M, Chiara M, Salza B, Quaranta L. Corso Grosseto viaduct: historical and technical overview. 10th international conference on bridge maintenance, safety and management (IABMAS 2020), June 28–July 2, 2020 (postponed to April 11–15, 2021), Sapporo, Japan. In: Yokota H, Frangopol DM, editors. Bridge maintenance, safety, management, life-cycle sustainability and innovations. London, UK: CRC Press/Balkema, Taylor & Francis Group; 2022.
22. Anghileri M, Biondini F, Rosati G, Savino P, Tondolo F, Sabia D, et al. Deconstruction of the Corso Grosseto viaduct and setup of a testing site for full scale load tests. 10th

international conference on bridge maintenance, safety and management (IABMAS 2020), June 28–July 2, 2020 (postponed to April 11–15, 2021), Sapporo, Japan. In: Yokota H, Frangopol DM, editors. Bridge maintenance, safety, management, life-cycle sustainability and innovations. London, UK: CRC Press/Balkema, Taylor & Francis Group; 2020.

23. Savino P, Tondolo F, Sabia D, Quattrone A, Biondini F, Rosati G, et al. Large-scale experimental static testing on 50-year-old prestressed concrete bridge girders. Appl Sci. 2023; 13(834):1–22.
24. Savino P, Quattrone A, Sabia D, Chiaia B, Tondolo F, Anghileri M, et al. Load tests on dismantled 50-year-old prestressed concrete bridge deck beams, 12th international conference on bridge maintenance, safety and management (IABMAS 2024), Copenhagen, Denmark, June 24-28, 2022. In: Jensen JS, Frangopol DM, Schmidt JW, editors. Bridge maintenance, safety, management, digitalization and sustainability. London, UK: CRC Press; 2024. p. 3484–92.
25. Tondolo F, Biondini F, Sabia D, Rosati G, Chiaia B, Quattrone A, et al. Experimental program and full-scale load tests on PC deck beams. In: Pellegrino C, Faleschini F, Zanini MA, Matos JC, Casas JR, Strauss A, editors. 1st conference of the European association on quality control of bridges and structures (EUROSTRUCT 2021), Padua, Italy, August 29–September 1, 2021. Lecture notes in civil engineering. Volume 200. Germany: Springer Science and Business Media; 2022.
26. Tondolo F, Sabia D, Chiaia B, Quattrone A, Savino P, Biondini F, et al. Full-scale testing and analysis of 50-year-old prestressed concrete bridge girders. 11th international conference on bridge maintenance, safety and management (IABMAS 2022), Barcelona, Spain, July 11–15, 2022. In: Casas JR, Frangopol DM, Turmo J, editors. Bridge safety, maintenance, management, life-cycle, resilience and sustainability. London, UK: CRC Press/Balkema, Taylor & Francis Group; 2022.
27. Beltrami C, Bianchi S, Cervio M, Anghileri M, Felicetti R, Quattrone A, et al. Bridge visual inspections: experience of local authorities and the case study of the Corso Grosseto viaduct. 10th international conference on bridge maintenance, safety and management (IABMAS 2020), June 28–July 2, 2020 (postponed to April 11–15, 2021), Sapporo, Japan. In: Yokota H, Frangopol DM, editors. Bridge maintenance, safety, management, life-cycle sustainability and innovations. London, UK: CRC Press/Balkema, Taylor & Francis Group; 2020.
28. Sabia D, Quattrone A, Tondolo F, Savino P. Dynamic identification of damaged PC bridge beams. 1st conference of the European association on quality control of bridges and structures (EUROSTRUCT 2021), Padua, Italy, August 29–September 1, 2021. In: Pellegrino C, Faleschini F, Zanini MA, Matos JC, Casas JR, Strauss A, editors. Lecture notes in civil engineering. Volume 200. Germany: Springer Science and Business Media; 2022.
29. Carsana M, Biondini F, Redaelli E, Valoti DO. On-site corrosion characterization of 50-year-old PC deck beams. 1st conference of the European association on quality control of bridges and structures (EUROSTRUCT 2021), Padua, Italy, August 29–September 1, 2021. In: Pellegrino C, Faleschini F, Zanini MA, Matos JC, Casas JR, Strauss A, editors. Lecture notes in civil engineering. Volume 200. Springer; 2022.
30. Carsana M, Valoti DO, Redaelli E, Biondini F. Corrosion assessment of 50-year-old PC deck beams. 11th international conference on bridge maintenance, safety and management (IABMAS 2022), Barcelona, Spain, July 11–15, 2022. In: Casas JR, Frangopol DM, Turmo J, editors. Bridge safety, maintenance, management, life-cycle, resilience and sustainability. London, UK: CRC Press/Balkema, Taylor & Francis Group; 2022.
31. Carsana M, Redaelli E, Valoti DO, Biondini F. Experimental campaign for corrosion assessment of 50-year-old PC deck beams. Eighth international symposium on life-cycle civil engineering (IALCCE 2023), July 2–6, 2023, Milan, Italy. In: Biondini F, Frangopol DM, editors. Life-cycle of structures and infrastructure systems. London, UK: CRC Press; 2023. p. 45–56.
32. Carsana M, Redaelli E, Biondini F. Corrosion investigations on PC deck beams of a 50-year-old decommissioned viaduct, 12th international conference on bridge maintenance, safety and management (IABMAS 2024), Copenhagen, Denmark, June 24–28, 2022. In: Jensen JS, Frangopol DM, Schmidt JW, editors. Bridge maintenance, safety, management, digitalization and sustainability. London, UK: CRC Press; 2024. p. 3476–83.
33. Anghileri M, Savino P, Capacci L, Bianchi S, Rosati G, Tondolo F, et al. Non-destructive testing and model validation of corroded PC bridge deck beams. 1st conference of the European association on quality control of bridges and structures (EUROSTRUCT 2021), Padua, Italy, august 29–September 1, 2021. In: Pellegrino C, Faleschini F, Zanini MA, Matos JC, Casas JR, Strauss A, editors. Lecture notes in civil engineering. Volume 200. Germany: Springer Science and Business Media; 2022.
34. Anghileri M, Rosati G, Biondini F, Savino P, Tondolo F. Experimental tests for mechanical characterization of prestressed concrete bridge deck beams. Eighth international symposium on life-cycle civil engineering (IALCCE 2023), July 2–6, 2023, Milan, Italy. In: Biondini F, Frangopol DM, editors. Life-cycle of structures and infrastructure systems. London, UK: CRC Press; 2023. p. 45–56.
35. Sabia D, Quattrone A, Tondolo F, Savino P. Experimental evaluation of the effect of controlled damages on the dynamic response of PC bridge beams. 11th international conference on bridge maintenance, safety and management (IABMAS 2022), Barcelona, Spain, July 11–15, 2022. In: Casas JR, Frangopol DM, Turmo J, editors. Bridge safety, maintenance, management, life-cycle, resilience and sustainability. London, UK: CRC Press/Balkema, Taylor & Francis Group; 2022.
36. Sabia D, Quattrone A, Savino P, Tondolo F. Dynamic response of PC bridge beams under different damages. Eighth international symposium on life-cycle civil engineering (IALCCE 2023), July 2–6, 2023, Milan, Italy. In: Biondini F, Frangopol DM, editors. Life-cycle of structures and infrastructure systems. London, UK: CRC Press; 2023. p. 45–56.
37. Sabia D, Quattrone A, Tondolo F, Savino P. Dynamic response of damaged precast bridge girders. 12th international conference on bridge maintenance, safety and management (IABMAS 2024), Copenhagen, Denmark, June 24–28, 2022. In: Jensen JS, Frangopol DM, Schmidt JW, editors. Bridge maintenance, safety, management, digitalization and sustainability. London, UK: CRC Press; 2024. p. 3476–83.
38. NTC2018; Aggiornamento delle "Norme tecniche per le costruzioni", S.O. alla G.U. n. 42 del 20 febbraio Serie generale. 2018.

39. Anghileri M, Biondini F. Validation of life-cycle-oriented computational methods for nonlinear analysis of RC/PC structures based on experimental tests. Struct Infrastruct Eng. 2025;21:1193–216.

AUTHOR BIOGRAPHIES

Francesco Tondolo, associate professor, Department of Structural, Geotechnical and Building Engineering, Politecnico di Torino, 10129, Torino, Italy. Email: francesco.tondolo@polito.it.

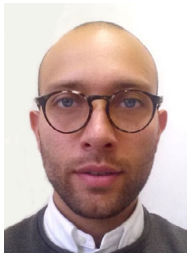

Pierclaudio Savino, PhD, Department of Structural, Geotechnical and Building Engineering, Politecnico di Torino, 10129, Torino, Italy. Email: pierclaudio.savino@polito.it.

Donato Sabia, associate professor, Department of Structural, Geotechnical and Building Engineering, Politecnico di Torino, 10129, Torino, Italy. Email: donato.sabia@polito.it.

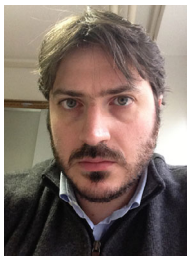

Antonino Quattrone, PhD, Department of Structural, Geotechnical and Building Engineering, Politecnico di Torino, 10129, Torino, Italy. Email: antonino.quattrone@polito.it.

Fabio Biondini, full professor, Department of Civil and Environmental Engineering, Politecnico di Milano, 20133 Milano, Italy. Email: fabio.biondini@polimi.it.

Gianpaolo Rosati, full professor, Department of Civil and Environmental Engineering, Politecnico di Milano, 20133 Milano, Italy. Email: gianpaolo.rosati@polimi.it.

Mattia Anghileri, PhD, Department of Civil and Environmental Engineering, Politecnico di Milano, 20133 Milano, Italy. Email: mattia.anghileri@polimi.it.

Bernardino Chiaia, full professor, Department of Structural, Geotechnical and Building Engineering, Politecnico di Torino, 10129, Torino, Italy. Email: bernardino.chiaia@polito.it.

How to cite this article: Tondolo F, Savino P, Sabia D, Quattrone A, Biondini F, Rosati G, et al. Large-scale tests of 50-year-old prestressed concrete bridge girders. Structural Concrete. 2026. https://doi.org/10.1002/suco.70488